

Synthesis of ZnO and ZnO : Mn Nanopowders by Ultrasonic Spray Pyrolysis

M.F. Bulaniy, V.Yu. Vorovsky, A.V. Kovalenko, O.V. Khmelenko

Oles Gonchar DNU, 72, Gagarina Ave., 49010 Dnipro, Ukraine

(Received 11 February 2016; published online 21 June 2016)

The paper analyzes the influence of the type of carrier gas: helium, air, nitrogen on the physical properties of ZnO and ZnO : Mn nanopowders synthesized by ultrasonic spray pyrolysis. It has been investigated the surface morphology of the samples, their crystalline quality and EPR spectra; the X-ray analysis has been conducted. The effect of heat treatment on the properties of nanocrystals has been studied. It is shown that ZnO : Mn nanopowders synthesized in a nitrogen atmosphere may have the *p*-type conductivity.

Keywords: Zinc Oxide, Ultrasonic spray pyrolysis method, Gas-transport: helium, air, nitrogen, Nanocrystals, Surface morphology of samples, Heat treatment, EPR spectra, Photoluminescence spectra, X-ray analysis.

DOI: [10.21272/jnep.8\(2\).02043](https://doi.org/10.21272/jnep.8(2).02043)

PACS number: 78.55.Et

Nanostructures based on ZnO possess luminescent, piezoelectric and ferromagnetic properties. These materials have high radiation, chemical and thermal resistance, a wide spectral window. They can possess both *n*- and *p*-type conductivity, are promising for producing radiating structures in the ultraviolet spectral region, gas sensors, elements of optoelectronics, devices of functional nanoelectronics and spintronics [1-3].

As known, zinc oxide is diamagnetic. The *n*-type conductivity is more typical for this material. Therefore, an actual technological problem during synthesis and doping processes is to obtain ZnO with the *p*-type conductivity. The difficulty of solving this problem lies in the fact that zinc oxide has a large number of natural point defects responsible for the *n*-type conductivity. It is also prone to the effect of self-compensation of the impurities causing the *p*-type conductivity. Upon doping, the acceptor impurities in ZnO tend to bind to crystal defects and form the electrically inactive complexes.

The authors of [4] shows the possibility to create the *p*-type conductivity in ZnO : Mn nanofilms on account of their doping with nitrogen. To obtain such films, the ultrasonic spray pyrolysis method was applied. At that, 0.5 molar aqueous solution (0.5 M) of zinc and manganese acetates was used, into which 2.5 M ammonium acetate was additionally added. According to the authors of the paper, doping with the acceptor impurity – nitrogen – leads to the substitution of oxygen ions by nitrogen ions in the ZnO crystal lattice and the appearance of the *p*-type conductivity in ZnO : Mn nanocrystals.

The ultrasonic spray pyrolysis method is based on the thermal decomposition of the solution, which contains the initial components of the synthesized material in the carrier gas flow [5]. The solid phase is formed due to evaporation of the solvent and thermolysis of the salts of the initial components in transport gas atmosphere. Therefore, in this synthesis method, there is the possibility of influencing the physical properties of ZnO nanocrystals by changing the transport gas type. Probably, an oxygen deficiency in the formation of the ZnO crystal lattice in an inert atmosphere can lead to the appearance of intrinsic defects of the acceptor type and the formation of the *p*-type conductivity in the obtained samples.

The aim of this work is to obtain ZnO and ZnO : Mn nanopowders with the *p*-type conductivity by ultrasonic

spray pyrolysis using various types of carrier gas.

An inert carrier gas – helium – was used at the first stage in the synthesis of pure ZnO nanopowder. At that, 2 types of ZnO nanopowders were synthesized from zinc nitrate solutions $Zn(NO_3)_2 \cdot 6H_2O$ with concentrations of 0.3 M and 0.03 M. The solutions were sprayed with an ultrasonic radiator operating at a frequency of 1.7 MHz. The spray particles (diameter is 1-5 μm) in the carrier gas flow (flow rate is 4.5 l/h) entered the furnace preheated to a temperature of $T = 650 \div 700$ °C. The time of thermal synthesis in the furnace was 7-10 s. The obtained ZnO nanopowder particles were separated from water vapor and other synthesis products using a stainless mesh filter heated to a temperature of $T = 150 \div 200$ °C. Images of the synthesized powder particles obtained by scanning electron microscope REMMA-102-02 are illustrated in Fig. 1. As seen from the presented images, the synthesized nanopowder particles have a spherical shape. The size of spherical particles decreases with decreasing concentration of zinc nitrate in the solution that corresponds to the conclusions of the work [5]. The diameter of spherical particles was found to be equal to 1.0-3.0 μm for the solution with zinc nitrate concentration of 0.3 M and 0.3-1.0 μm for the solution with zinc nitrate concentration of 0.03 M, respectively (Fig. 1). X-ray diffraction studies of the powders performed on the diffractometer DRON-2.0 showed that ZnO nanopowders have a crystal structure of the wurtzite type. Estimation of the average sizes of ZnO nanocrystals, done by the Scherrer method [6, 7], showed that for these substances concentrations the average sizes of the crystals, which are the constituents of spherical particles, are equal to $d \sim 56$ nm and $d \sim 37$ nm, respectively.

The doping process and synthesis of ZnO : Mn nanopowder were carried out from zinc nitrate solution with a concentration of 0.3 M, into which manganese nitrate ($Mn(NO_3)_2 \cdot 6H_2O$) was added in an amount corresponding to the manganese ion concentration of 0.01 M. At first, the samples doped with Mn were obtained in an inert medium with the carrier gas helium. As a result of thermal decomposition of a solution containing zinc and manganese nitrates, the powder particles are formed (their external view is illustrated in Fig. 1c. The data on the study of the morphology of the obtained articles allows to conclude that ZnO : Mn powder particles retained a

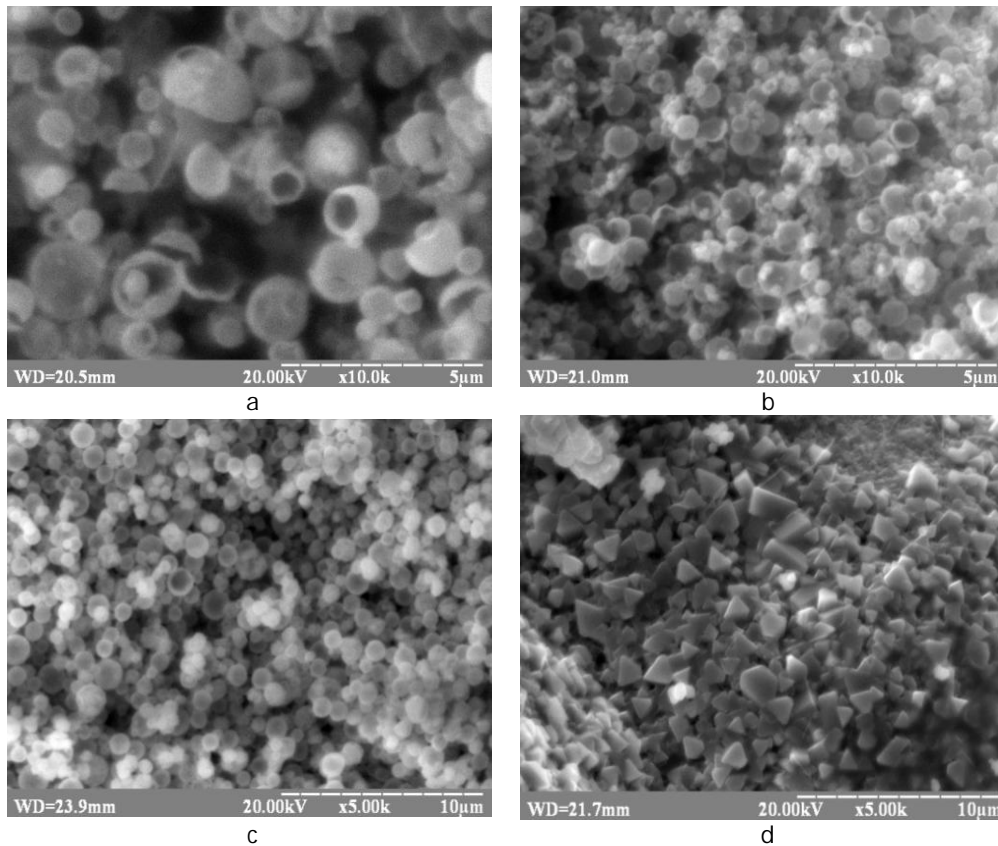


Fig. 1 – External view of the ZnO powder particles obtained from the solution containing zinc nitrate with concentrations of 0.3 M (a) and 0.03 M (b), as well as the ZnO : Mn powder particles obtained from the solution containing zinc nitrate with a concentration of 0.3 M and manganese nitrate with a concentration of 0.01 M before (c) and after (d) annealing in environment

spherical shape. The average size of spherical particles was found to be approximately equal to $\sim 1 \mu\text{m}$ that, in turn, is smaller than the sizes of spherical particles of pure ZnO nanopowder with the same concentration of zinc nitrate in a solution (see Fig. 1).

It was important from the technological point of view to determine the possibility of doping ZnO nanopowder with Mn ions during synthesis. To establish the fact of doping, the EPR spectra of the obtained nanopowders were studied. These studies showed that doping of ZnO powder with manganese ions in the synthesis, when the carrier gas helium is used, does not occur. Subsequent annealing of the powder in helium at a temperature of $T = 800 \text{ }^\circ\text{C}$ during 1 h also does not lead to doping. Only after annealing of the samples in air at a temperature of $T = 800 \text{ }^\circ\text{C}$ during 1 h, six characteristic lines of the hyperfine Mn^{2+} ion structure were revealed in the EPR spectra that indicates doping of ZnO crystals with Mn ions. Thus, ZnO : Mn nanocrystals were obtained only after heat treatment. The observed EPR spectrum for the Mn^{2+} impurity in ZnO has the following parameters: spectroscopic splitting factor $g = 2.001$, hyperfine structure constant $A = 65.94 \text{ Oe}$. These parameters are typical for Mn^{2+} ions in the hexagonal zinc oxide lattice [8].

The external view of the ZnO : Mn powder particles after annealing in air is shown in Fig. 1d. Analysis of the obtained results allows to conclude that after annealing of the powder particles, its recrystallization occurred, as a result of which crystals of various growth forms were formed of spherical particles. The average crystal size was found to be equal to $\sim 1\div 2 \mu\text{m}$, and the crystallite size,

of which they consist, increased to a value of $d \sim 120 \text{ nm}$. This fact predetermined the changes in the photoluminescence spectra of nanopowders (Fig. 2).

A low intense, weakly structured photoluminescence spectrum concentrated in the green-blue spectral region of the initial ZnO : Mn nanopowder indicates great imperfection of the crystal structure of the samples (Fig. 2a). After annealing in an oxygen-containing medium as a result of recrystallization, increase in the size of individual crystals, the degree of their imperfection decreased, and the crystal structure became more perfect. Hence, the radiation intensity increased, and the photoluminescence spectrum became more structured and is concentrated,

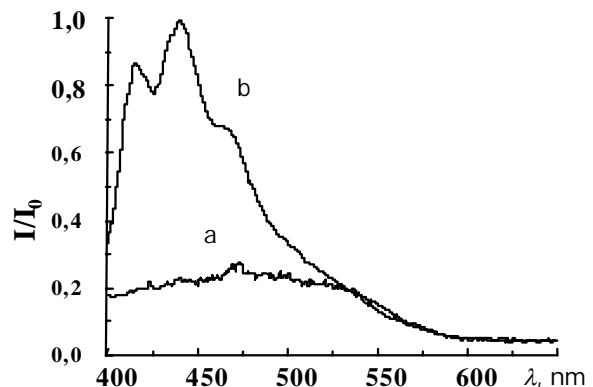


Fig. 2 – Photoluminescence spectra of the initial ZnO : Mn nanopowder with concentrations in the solution of zinc nitrate of 0.3 M and manganese nitrate of 0.01 M synthesized in helium atmosphere before (a) and after (b) annealing in the environment

mainly, in the blue spectral region (Fig. 2b). Now, it is possible to separate three radiation maxima in the spectrum: $\lambda_{\max} \sim 416$ nm, which is probably associated with the radiative recombination in the donor-acceptor pair, and also $\lambda_{\max} \sim 441$ nm and $\lambda_{\max} \sim 470$ nm, which are associated with the complexes including impurities and intrinsic defects [9].

Further, we performed studies of the synthesis process of ZnO nanopowders and their doping with manganese using other carrier gases: air and nitrogen. Aqueous solutions for the synthesis had the following compositions: $\text{Zn}(\text{NO}_3)_2 \cdot 6\text{H}_2\text{O}$ with a concentration of 0.3 M and $\text{Mn}(\text{NO}_3)_2 \cdot 6\text{H}_2\text{O}$ with a concentration of 0.01 M. The synthesis temperature was equal to $T = 670$ °C.

The powders synthesized with different carrier gases were also subjected to annealing at the temperature of $T = 800$ °C in air during 1 hour. The obtained samples were studied by the EPR and X-ray diffraction analysis methods (see Fig. 3).

The results obtained allow to conclude that in both cases six characteristic lines of a hyperfine structure of Mn^{2+} paramagnetic impurity are already present after synthesis in the EPR spectra of ZnO : Mn nanopowders that proves the fact of doping during the synthesis. After annealing intensity of these lines and area under the resonance curve increase that implies an additional introduction of Mn^{2+} paramagnetic impurity into the ZnO crystal lattice.

The reflex of the secondary $\beta\text{-MnO}_2$ phase (angle is $2\theta = 26.7$ degrees) is present on the electron diffraction pattern of the ZnO : Mn nanopowder synthesized in air atmosphere. The secondary phase disappears after annealing in air. ZnO : Mn nanopowder becomes a single-phase with a crystal structure of the wurtzite type. Here, excess manganese is embedded in ZnO crystal lattice that is confirmed by the study of the EPR spectra. It can be concluded based on the X-ray pattern shown in Fig. 3

that ZnO : Mn nanopowder synthesized in the nitrogen atmosphere contains an additional $\alpha\text{-MnO}_2$ phase (angle $2\theta = 19.0$ deg.), which disappears after annealing in air.

The data presented in Fig. 3 implies that a wide absorption line with $g = 4.2874$ appears in the EPR spectrum of ZnO : Mn nanopowder when using carrier gas nitrogen in the region of small magnetic fields. The presence of this line is associated with the formation in ZnO of defects arising when crystals are formed in an inert medium with oxygen deficiency and, possibly, due to the introduction of nitrogen atoms into the crystal lattice. Such defects, based upon the magnitude of the g factor, are the acceptor centers, therefore, ZnO : Mn powder can have the p -type conductivity. After annealing in air of ZnO : Mn nanopowder, the specified defects disappear, zinc oxide is oxidized, and, thus, the line with $g = 4.2874$ disappears in the EPR spectrum. It retains only six lines of a hyperfine structure of the EPR spectrum of Mn^{2+} ions. After such heat treatment, as a result of decreasing imperfection, we should expect an improvement in the crystalline quality of the synthesized material that was confirmed by further studies. The performed X-ray diffraction analysis showed a change in the crystal lattice parameters of ZnO nanopowder (parameters a , c) before and after doping with Mn under various synthesis conditions. In Table 1 we present the results of the corresponding calculations for ZnO and ZnO : Mn nanopowders with a concentration of manganese nitrate in the solution of 0.01 M synthesized with different carrier gases, before and after annealing in air atmosphere. The average crystal size in these nanopowders is estimated. As seen from Table 1, the crystal lattice parameter of ZnO : Mn nanopowder significantly increased relative to the value of this parameter $a = 3.2415$ Å for pure ZnO nanopowder. After annealing at the temperature of $T = 800$ °C during 1 h, parameter a decreases, but it is still greater than that for pure ZnO powder.

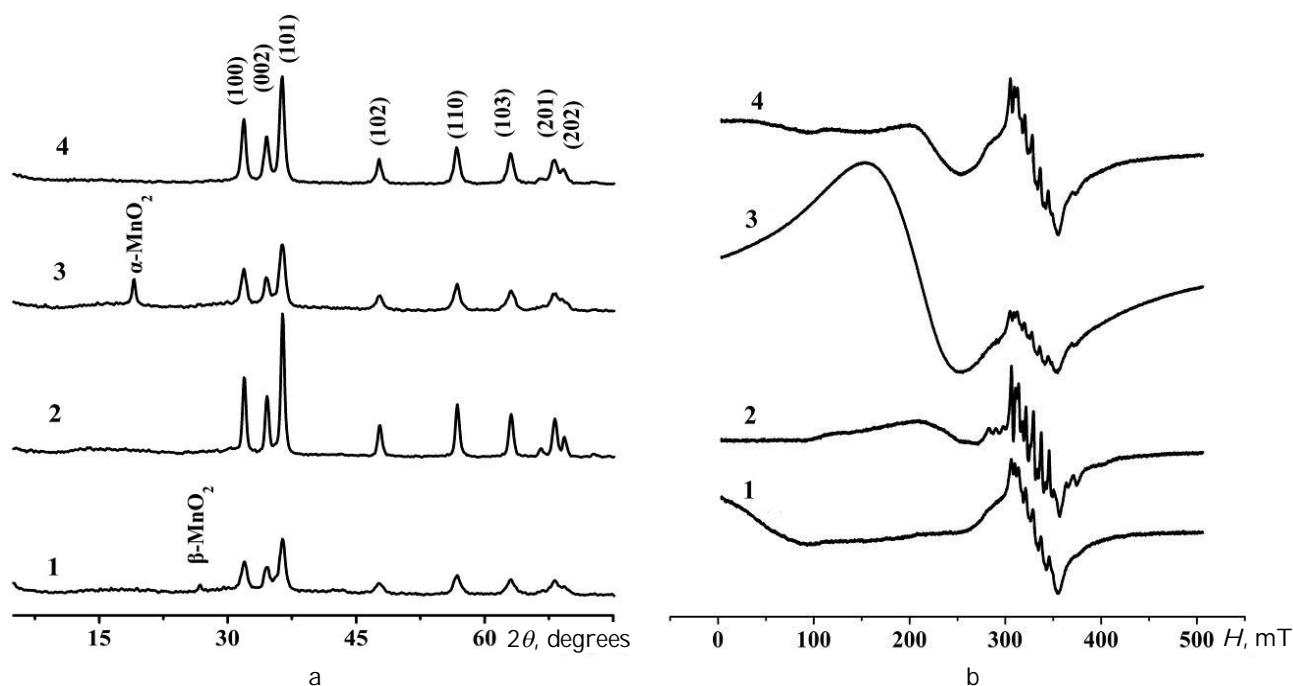


Fig. 3 – X-ray patterns of ZnO : Mn nanopowders (a) and their EPR spectra (b) obtained with the carrier gas air before (1) and after (2) annealing, as well as the obtained with the carrier gas nitrogen before (3) and after (4) annealing in air

Table 1 – Crystal lattice parameters and crystal sizes of the studied ZnO nanopowders

No	Nanopowder type	Carrier gas: air				Carrier gas: nitrogen			
		Parameters, Å		d , nm	c/a	Parameters, Å		d , nm	c/a
		a	c			a	c		
1	ZnO	3.2415	5.1946	56.0	1.6025	3.2389	5.1932	38.0	1.6034
2	ZnO : Mn before annealing	3.2431	5.1972	32.0	1.6025	3.2458	5.1961	35.0	1.6009
3	ZnO : Mn after annealing	3.2399	5.1936	70.0	1.6015	3.2441	5.1930	48.0	1.6007

Table 2 – Density of dislocations in ZnO and ZnO : Mn nanopowders

No	Carrier gas type	Density of dislocations in nanopowders, $D \times 10^{10} \text{ cm}^{-2}$					
		ZnO	ZnO : Mn (0.01 M)	ZnO : Mn (0.01 M) after annealing	ZnO : Mn (0.02 M)	ZnO : Mn (0.04 M)	ZnO : Mn (0.16 M)
1	Air	35.8	45.0	12.4	49.2	62.5	98.6
2	Nitrogen	45.2	53.0	26.4	57.7	87.1	140.1

As known, a change in the ratio of the crystal lattice parameters (ca) of zinc oxide compared with the value of this ratio for an ideal crystal lattice is the criterion of structural perfection. Monocrystalline ZnO obtained under equilibrium conditions crystallizes in the wurtzite structure with the unit cell parameters: $a = 3.249 \text{ Å}$, $c = 5.205 \text{ Å}$ and $ca = 1.6020$ [10]. Comparing the ratios ca given in Table 1, it can be concluded that ZnO : Mn nanopowders synthesized in a nitrogen atmosphere have the value of ca which is much less than the equilibrium one. This fact is a sign of imperfection of the crystal lattice of ZnO : Mn nanocrystals.

An important indicator of perfection of the substance crystal lattice is the presence in it of dislocations, whose density depends on the conditions of the crystallization process. It is shown in [11] that the dislocation density is $D \sim 10 \text{ cm}^{-2}$ in ZnO single-crystals obtained under equilibrium conditions by the hydrothermal method at a growth rate of 0.01-0.1 mm per day. In the crystals obtained by the gas-phase method under non-equilibrium conditions and a growth rate in the range of 0.1-0.2 mm per day, the dislocation density is $D \sim 104 \text{ cm}^{-2}$. As X-ray diffraction analysis shows, the dislocation density of ZnO nanocrystals obtained by spray pyrolysis is six orders of magnitude higher. The data on the dislocation density of

pure ZnO nanopowder and doped ZnO : Mn nanopowders at different manganese concentrations for carrier gases air and nitrogen are given in Table 2.

Thus, the results obtained confirm the fact that the crystallization conditions are characterized by an increased level of non-equilibrium, formation of a large number of dislocations in the synthesis of ZnO nanopowders by the spray pyrolysis method. Doping of ZnO nanopowder with Mn leads to a further increase in the number of dislocations. The synthesis of ZnO : Mn nanopowder in a nitrogen medium stimulates this process: in this case, the number of dislocations becomes larger than in the synthesis of ZnO : Mn nanopowder in an oxygen-containing medium. In connection with this, it can be asserted that the oxygen deficiency in the formation of the ZnO crystal lattice in an inert nitrogen atmosphere increases the number of intrinsic defects and, probably, due to the introduction of nitrogen atoms into the crystal lattice results in the formation of acceptor centers in the obtained samples. The results of the work performed show that in the synthesis and doping of zinc oxide with manganese by the spray pyrolysis method, the carrier gas type significantly influences the physical properties of the nanocrystals, and ZnO : Mn nanopowder synthesized in a nitrogen atmosphere can have the p -type conductivity.

REFERENCES

1. S. Kasap, P. Capper, *The Springer Handbook of Electronic and Photonic Materials* (Berlin: Springer: 2007).
2. D.D. Awschalom, D. Loss, N. Samarth, *Semiconductor Spintronics and Quantum Computation* (Berlin: Springer: 2002).
3. Yu.A. Danilov, Ye.S. Demidov, A.A. Yezhevskiy, *Novyye magnitnye materialy i pribory na ikh osnove. Uchebnoye posobiye* (Nizhniy Novgorod: NGU: 2010).
4. V.O. Pelenovich, Sh.U. Yuldashev, A.S. Zakirov, *Physica B* **404**, 5266 (2009).
5. V.V. Pankov, *Vestnik BGU* 2 No 2, 3 (2007).
6. A.L. Patterson, *Phys. Rev.* **56**, 978 (1998).
7. S.S. Gorelik, Yu.A. Skakov, L.N. Rastorguyev, *Rentgenograficheskiy i elektronno-opticheskiy analiz* (M.: MISIS: 1994).
8. M.V. Vlasova, N.G. Kakazey, A.M. Kalinichenko, A.S. Litovchenko, *Radiospektroskopicheskiye svoystva neorganicheskikh materialov* (K.: Nauk. dumka: 1987).
9. E.V. Kortunova, V.I. Lyutin, *Gidrotermal'nyye monokristally tsinkita. Issledovaniye fizicheskikh svoystv. Sbornik, tom 1* (Aleksandrov: VNIISIMS: 2000).
10. V.I. Gavrilenko, A.M. Grekhov, D.V. Korbutyak, V.G. Litovchenko, *Opticheskiye svoystva poluprovodnikov. Spravochnik* (K.: Nauk. dumka: 1987).
11. M.M. Mezdrogina, E.Yu. Danilovskiy, R.V. Kuzmin, *Semiconductors* **44**, 321 (2010).